Int. J. Mech. Eng. Autom.
Volume 1, Number 4, 2014, pp. 193-202
Received: July 6, 2014; Published: October 25, 2014

International Journal of
Mechanical Engineering
and Automation

Dynamic Analysis and Shape Optimization of Automotive Gage Panel

Alexander Janushevskis[1], Anatoly Melnikovs[1] and Janis Janusevskis[2]

1. Machine and Mechanism Dynamics Research Lab, Riga Technical University, Riga LV-1006, Latvia

2. Institute of Mechanics, Riga Technical University, Riga LV-1006, Latvia

Abstract: Design of mechanical products nowadays extensively utilizes simulation models which allow fast design procedure. FEM models are often used for optimization in metamodel based methods. In this work automotive GP (gage panel) is designed using FEM and metamodel based optimization. The complex geometrical model of the GP initial design is created by CAD software and simplified FEM model is used for required dynamic and static FEM calculations. The lowest 10 natural frequencies, distribution of stresses, strains and displacements under static loading of the GP, as well as the stationary and transient behaviors under deterministic and random excitations of the GP are investigated. In the next step, these results are taken into account for optimization problem formulation. The optimum cross section shapes of the GP brackets are found using metamodel based shape optimization combined with effective parameterization. The employed parameterization is based on knot points of non-uniform rational B-splines allowing reduction of the number of design parameters. Calculation of the responses of the full FEM models is based on Latin Hypercube design of experiments. Quadratic locally weighted polynomial metamodels are used for fast optimization procedure. The bracket optimum design improves overall characteristics of the GP as it has higher fundamental frequency, improved strength and stiffness properties.

Key words: Gage panel, dynamic analysis, metamodel, shape optimization, finite element, design of experiments.

1. Introduction

Always actual is a problem of safe and environmentally friendly engineering object development which has high functional properties, attractive style and competitive price. Automotive gage panels must meet many requirements [1-2] starting with appropriate styling and precisely measurable functional characteristics such as stiffness, weight, eigenfrequencies, accuracy, stress and deformation levels under different loading conditions etc. In this work, mechanical design of automotive GP is discussed.

In Fig. 1, we can see the initial 3D model of GP designed for a passenger car. Frame components of GP are manufactured by injection molding. The conventional plastics ABC and PMMA are used as materials. Standard electronic parts are taken for GP devices, but electronic board has original design.

In the first step, the geometrical 3D model is created by CAD software SW (SolidWorks). The main inertial properties of GP such as mass, moments of inertia, center of mass, as well as volume, surface area and others are calculated. Mass of the initial GP assembly is $m_0 = 1.27$ kg and volume of the plastic part with brackets is $v_0 = 168{,}000$ mm^3. GP has complex design with a large number of components (especially electronic board elements), FE model has large number of DOF and it is difficult to use in optimization loop. The GP design was simplified for FE analysis and, as result, GP model consists of only 21 main parts: 5 deformable frame parts and 16 other rigid body components that take into account the inertial characteristics of the internal devices. Respectively, small parts like electronic elements, which cannot considerably affect GP dynamics, are not taken into account.

Corresponding author: Alexander Janushevskis, Dr.Sc.Ing, professor, research fields: CAD/CAE, design of experiments and optimization. E-mail: janush@latnet.lv.

GP model is meshed with parabolic tetrahedral elements (~360000 DOF). The resulting mesh is shown in Fig. 2. The FE mesh is generated with curvature based mesh (max elements size is 7.5 mm, min element size is 1.6 mm, element size growth ratio is 1.5) which ensures accurate discretization of the complex shapes of the GP bodies. FE analysis is used to evaluate different responses of GP: Maximal von Mises stress in the material from impact loading; maximal displacements and accelerations at the characteristic points of GP in stationary and transient vibration processes due to polyharmonic excitations as well as dispersions of the appropriate vibrational characteristics in the case of random excitations; natural frequencies of the GP.

The static, frequency, harmonic, modal time history and random vibrations analyses characterizing quality of GP are given in Sections 2-6, respectively. In Section 7, GP bracket shape optimization procedure is discussed in details. The conclusions are summarized in Section 8.

2. Strength Calculation of GP

Generally the strength of GP designs is checked using special vibrostands. The natural prototype of GP is subjected to different dynamic loads. Vibrostability and vibration strength of the GP are checked on excitations in the frequency domain from 10 to 410 Hz. One of the main natural experiment is a test of shock resistance of the GP design under acceleration level a = 10 g. Such experiments require significant material and time expenses and for optimization purposes the computer based design check must be used.

Fig. 1 Frontal and back view of GP.

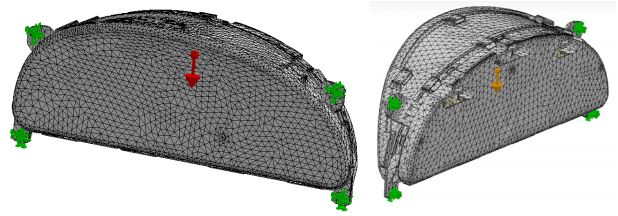

Fig. 2 Frontal and back view of meshed GP model.

As we can see in Fig. 2, the model of the GP is fixed with 4 brackets and acceleration acts in the vertical direction. For the initial design of the GP the maximal von Mises stresses from impact loading are presented in Fig. 3. The most loaded places, where von Mises stress level is greater than 3 MPa, are shown in red. We can see that maximal stresses are concentrated near the lower brackets and at the fixings of the transparent screen component: the stress level reaches 4 MPa. Other components of the GP have considerably less stress levels. The side view of the deformed shape (scale up 200 times) of the GP and resultant displacements URES are presented in Fig. 4. The upper part of GP screen is twisted and has maximal displacements. We can see maximal deformations (Fig. 4 left) near the brackets and at the screen fixings where tensile stresses are acting.

3. Frequency Analysis of GP

Frequency analysis was carried out to find natural frequencies of the GP model and evaluate possible resonance in the case of external excitation. The same FE mesh for model as considered before is used. The contacts between assembly's parts are defined as bonded. The numerical solver FFEPlus of SW Simulation is used for calculations of the 10 lower natural frequencies. The obtained results (Table 1) show that fundamental frequency of the GP is sufficiently

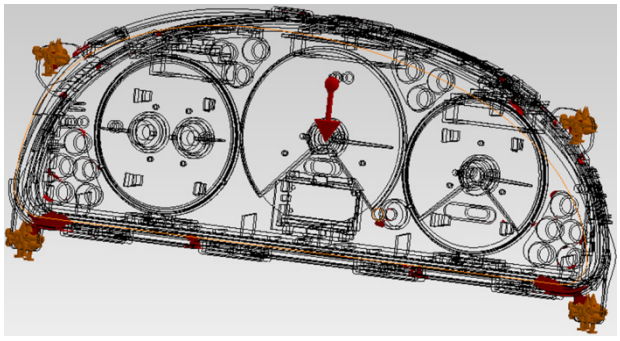

Fig. 3 Most loaded places of the GP from impact loading.

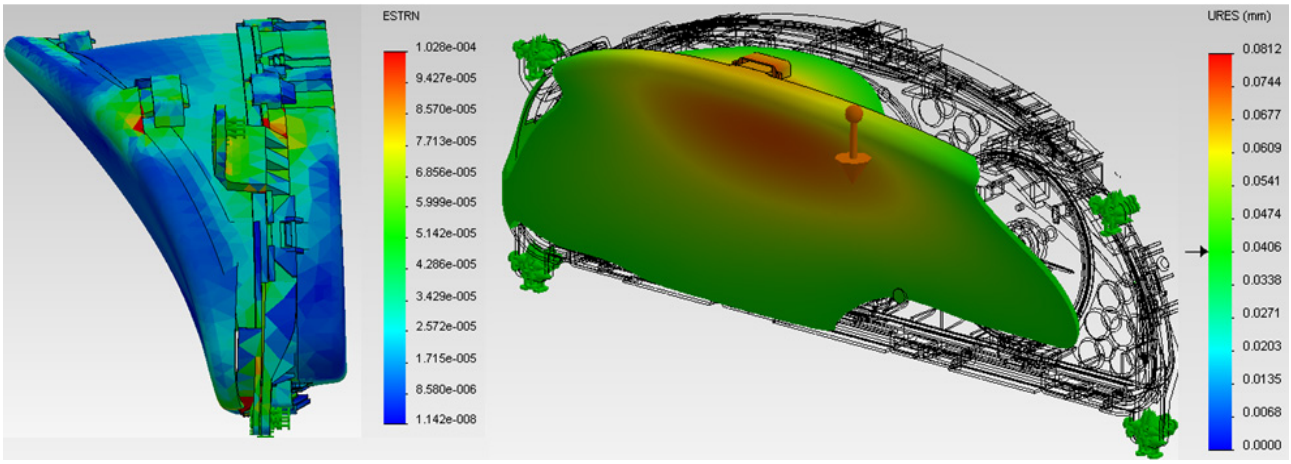

Fig. 4 Deformation (left) and displacements (right) of the GP from impact loading.

Table 1 Natural frequencies of the GP.

No.	Frequency (Hz)
1	140.14
2	182.09
3	194.28
4	241.69
5	248.28
6	296.52
7	308.43
8	314.49
9	328.31
10	332.43

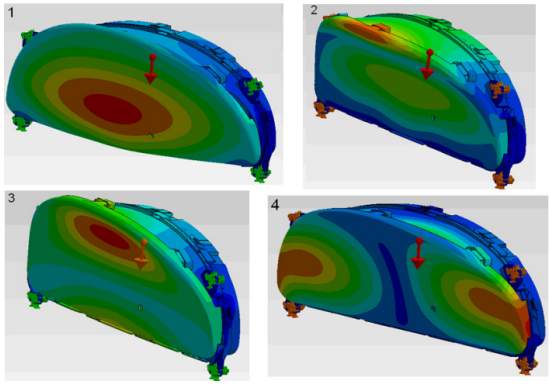

Fig. 5 The four lower natural modes of the GP.

high f_1 = 140.14 Hz. The obtained mode shapes for the GP are shown in Fig. 5. The red color shows the regions with maximal and blue with minimal displacements. We can see that there is a high density of natural frequencies—10 frequencies are acting in the 192 Hz interval. Consequently, any of the lower frequencies can play an important role in the GP vibrations.

4. Harmonic Analysis of GP

Possible vibration levels of the GP are checked for harmonic excitations in the frequency domain from 1 to 500 Hz. Harmonic excitations (a = 10 g) are applied to the GP supports with vertical direction of action. The modal damping ratio was determined from proper GP field tests. The solution points are clustered around each natural frequency to capture the response accurately at these frequencies neighborhood.

The responses are calculated at the prescribed locations of the GP to reduce necessary computational recourses. These points are situated at the centers of 4 measuring devices (Fig. 6: points 1-4). As was shown before in the static calculation, maximal stresses occur in the regions of the lower brackets and at the transparent screen fixings of the GP (Fig. 3). Additionally three stress response points are also defined (Fig. 6: points 5-7).

The amplitudes of the resultant displacements are presented in Fig. 7. We can see that significant magnitudes of GP vibrations are obtained on the first and third resonance frequencies. The second frequency does not show peak. Certainly, bigger amplitudes occur on the devices points 2-3 with locations farther from GP bracket. Figs. 8-10 show the displacement components in the directions X, Y and Z respectively. The results indicate that vibration amplitudes in the direction Z are bigger on the first and third resonance frequencies and reach 0.355 mm. Comparison of maximal resultant displacements in quasi-static (Fig. 3

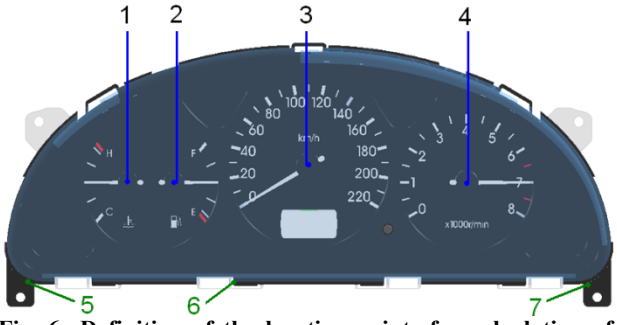

Fig. 6 Definition of the location points for calculation of responses.

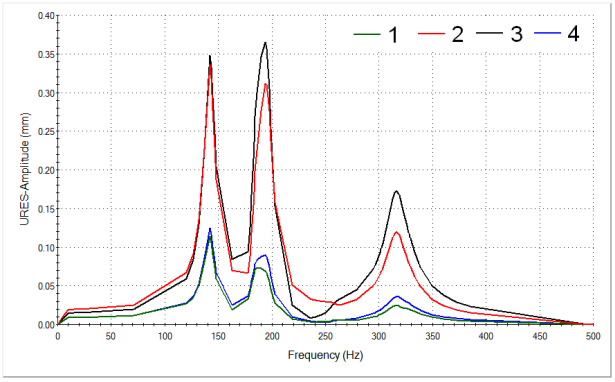

Fig. 7 Amplitudes of the resultant displacements at the defined 4 points of the GP.

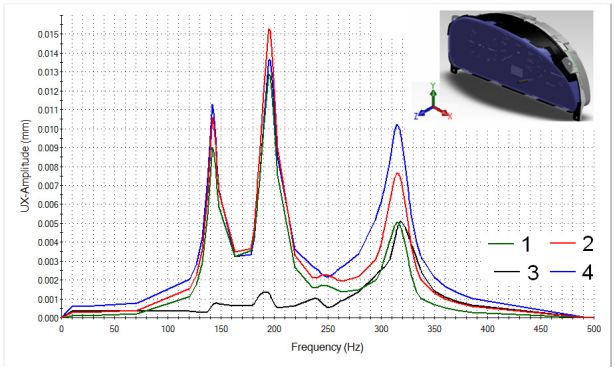

Fig. 8 Amplitudes of UX displacements at the defined 4 points of the GP.

right) and dynamic (Fig. 7) cases show that dynamic amplitudes have more than 4.5 times greater values.

In Fig. 11, von Mises stress levels are presented in the frequency range. The highest level of stress is at the point 6 of the transparent plastic screen fixture. It occurs for the eighth natural frequency when the stress value is 1.45 times bigger than in previously discussed quasi-static case (Fig. 3). As we can see, eighth frequency is mainly contributing in the Z and Y directions. Important part of the stresses is taken by the

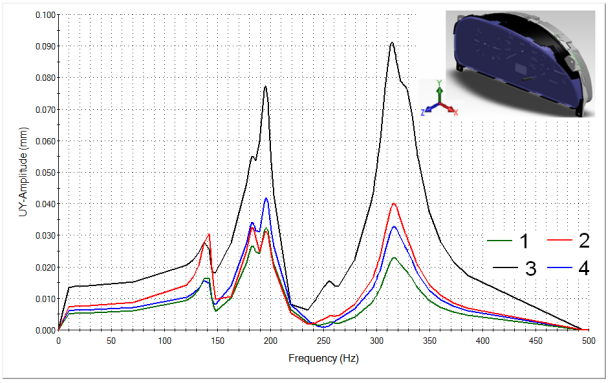

Fig. 9 Amplitudes of UY displacements at the defined 4 points of the GP.

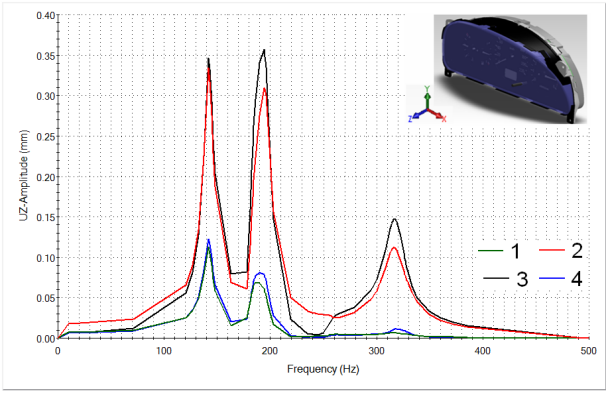

Fig. 10 Amplitudes of UZ displacements at the defined 4 points of the GP.

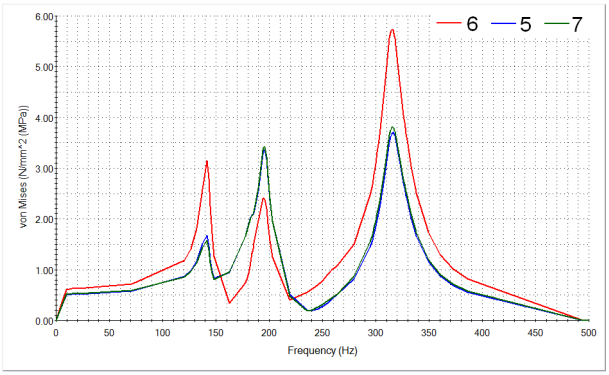

Fig. 11 von Mises stresses at the defined 3 points of the GP.

brackets 90 degree angle between the bracket and the GP body. At the points 5 and 7 (Figs. 6 and 11) material is subjected to tensile forces. The direction of vibration play important role. It is interesting that excitations with lower frequencies give smaller stress levels.

5. Modal Time History Analysis of GP

Also transient behavior of the GP is calculated from

vibrational excitation. It is assumed that polyharmonic excitations act on the GP brackets:

$$f(t) = A\sin(wt + \alpha) + B\cos(2wt + \beta) \quad (1)$$

where frequency ω is equal with fundamental frequency, but amplitudes A and B, respectively 50 and 40 m/s^2 and $\alpha = \pi/2$; $\beta = 0$.

Newmark method is used for integration with step size 0.01 s from zero initial conditions.

Response curves for vertical displacement are presented in Fig. 12. We can see that maximal amplitudes of vertical displacement are observed on the central device 3 of the GP.

6. Random Vibrations Analysis of GP

Random vibration analysis are used to calculate the response due to non-deterministic loads, such as, loads generated on the wheels of a car traveling on a rough road. Loads are described statistically by PSD (Power Spectral Density) functions. They act at the supports as a vertical uniform base excitation. PSD function curve is taken from Standard MIL-STD-810F [3]. The frequency domain is from 10 to 500 Hz.

As one can see in Fig. 13 1st, 3rd and eighth frequencies give important contribution. Comparing PSD of von Mises amplitudes ratio of the point 6 with other points 5 and 7 (Figs. 11 and 14), domination of the eighth frequency increases in random vibration analysis.

7. GP Bracket Shape Optimization

For topology and shape optimization of structures the different realizations of homogenization method are

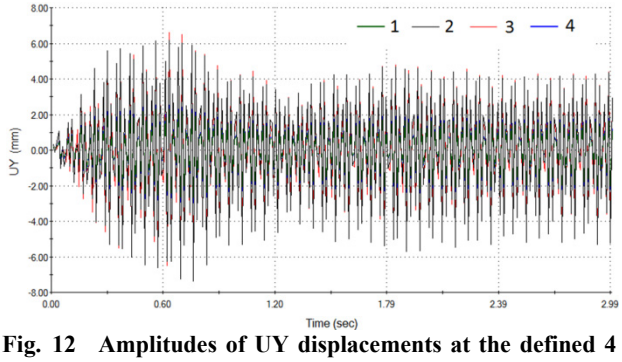

Fig. 12 Amplitudes of UY displacements at the defined 4 points of the GP.

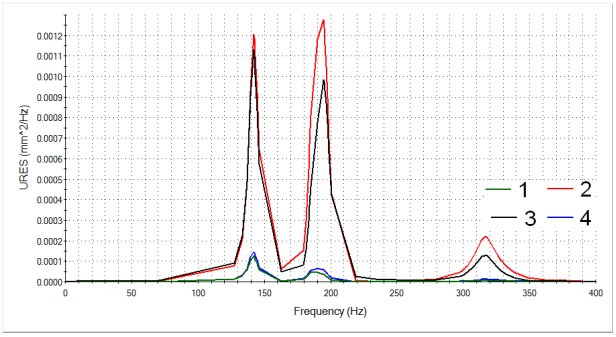

Fig. 13 PSD of vertical URES displacements at the defined points of the GP.

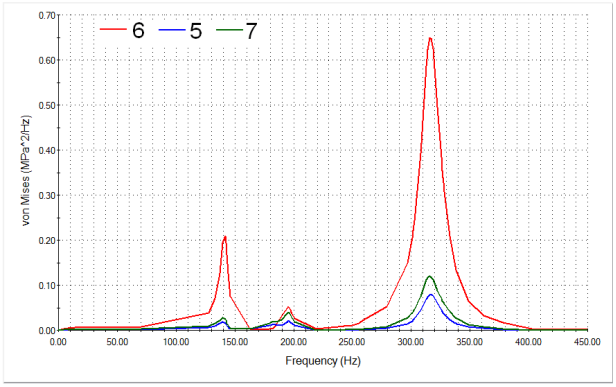

Fig. 14 PSD of von Mises stress at the defined points of the GP.

vastly used [4-5]. This method is highly effective for shell constructions. The basic idea of this method is to consider each FE of the mechanical system model as a composite consisting of material and void. The ratio of material volume to void is sought in the FE to maximize the defined criteria, for example, the following performance indicator:

$$PI = \frac{\sigma_{0,\max} v_0}{\sigma_{i,\max} v_i} \quad (2)$$

where $\sigma_{0,\max}$ is the maximum equivalent stress value of the original design, v_0 is a design starting volume, $\sigma_{i,\max}$ and v_i are the values of variables obtained in the i-th iteration.

This method was successfully applied for optimization of the automotive designs made from isotropic material [6]. However it is very time consuming procedure because number of the design parameters can reach million and more. In the case of solid bodies it frequently produces shapes that are difficult to manufacture. As shown in Ref. [7], the

Hybrid Cellular Automata method does not allow parallelization of computations and PBS queuing system has been used.

The shape optimization approach based on metamodeling [2, 8] is used to reduce necessary time and other resources. It includes following 6 steps:

(1) Planning the position of the control polygon or knot points of NURBS (Non-Uniform Rational B-Splines) which can define curves for creating smooth shapes of 3D object in CAD environment. Coordinates of the position of these points are independent variables or factors for DOE (Design of Experiments). The interval boundaries or side constraints of factors are chosen in accordance with appropriate object size, constructive and technological possibilities or other important considerations. The variables domain should include possible optimal solution, otherwise optimization process must be repeated in loop, adjusting interval boundaries for factors;

(2) Creating of geometrical models of 3D object using CAD software in conformity with DOE. During this step it is possible obtain volume, mass and other inertial characteristics of model that could be used for optimization;

(3) Calculating of responses for complete FEM model using CAE software. This model of object must ensure sufficient accuracy for responses;

(4) Creating metamodels (surrogate models) for responses obtained in previous step on the basis of experiment. Accuracy of approximations and prediction errors must be estimated. If results are satisfactory, then proceed with the next step, otherwise try to improve metamodel accuracy;

(5) Using metamodels for shape optimization, i.e., extremum of subsequent objective function is searched by global stochastic search procedures taking into account known constraints;

(6) Validating the optimal design using CAE software for the complete FEM model. Optimal values of factors are used for creation of the optimal shape of 3D object model in CAD software.

In this specific situation, one of the solutions for improving the GP reliability could be increasing of the GP bracket cross-section thickness and changing shape at the most loaded place. The cross-section shape for bracket's strengthening is defined by the 3 knot points (Fig. 15a) of NURBS. Design parameters are coordinates of the knot points varied in the following ranges: $3 \le X1 \le 9$; $1.5 \le X2 \le 6$; $1 \le X3 \le 3$. As a cross-section profile is defined, the 3D-shape is created using the path curve (Fig. 15b). The same shape for strengthening is created on the second bracket of the GP frame component.

The design of experiments for 3 factors and 40 trial points is used (Fig. 16) with MSE (Mean-Square Error) criterion [9-10] by EDAOpt [11]—software for design of experiments, approximation and optimization developed in Riga Technical University. This design of experiment also is available at http://www.mmd.rtu.lv.

The geometrical models are developed by SW for all variants. In the next step responses of these models are calculated by SW Simulation. Then these responses are used for approximation by EDAOpt. For example, the following expression is used for approximation of response y by quadratic polynomial:

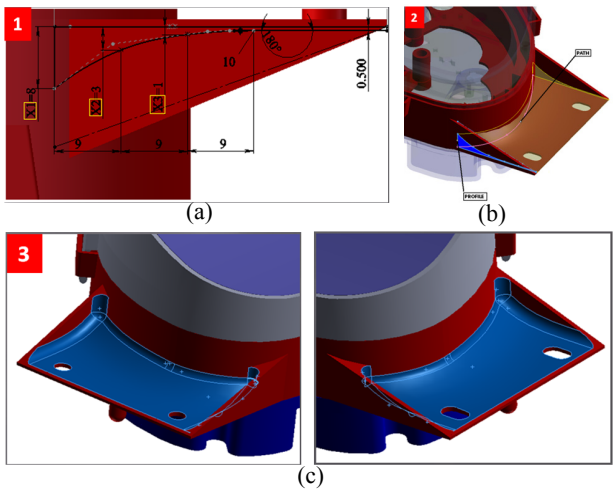

Fig. 15 The parameterization of brackets shapes: (a) Cross-section shape definition with NURBS; (b) 3D-shape creation through path curve; (c) additional fillets and obtained shapes of GP brackets.

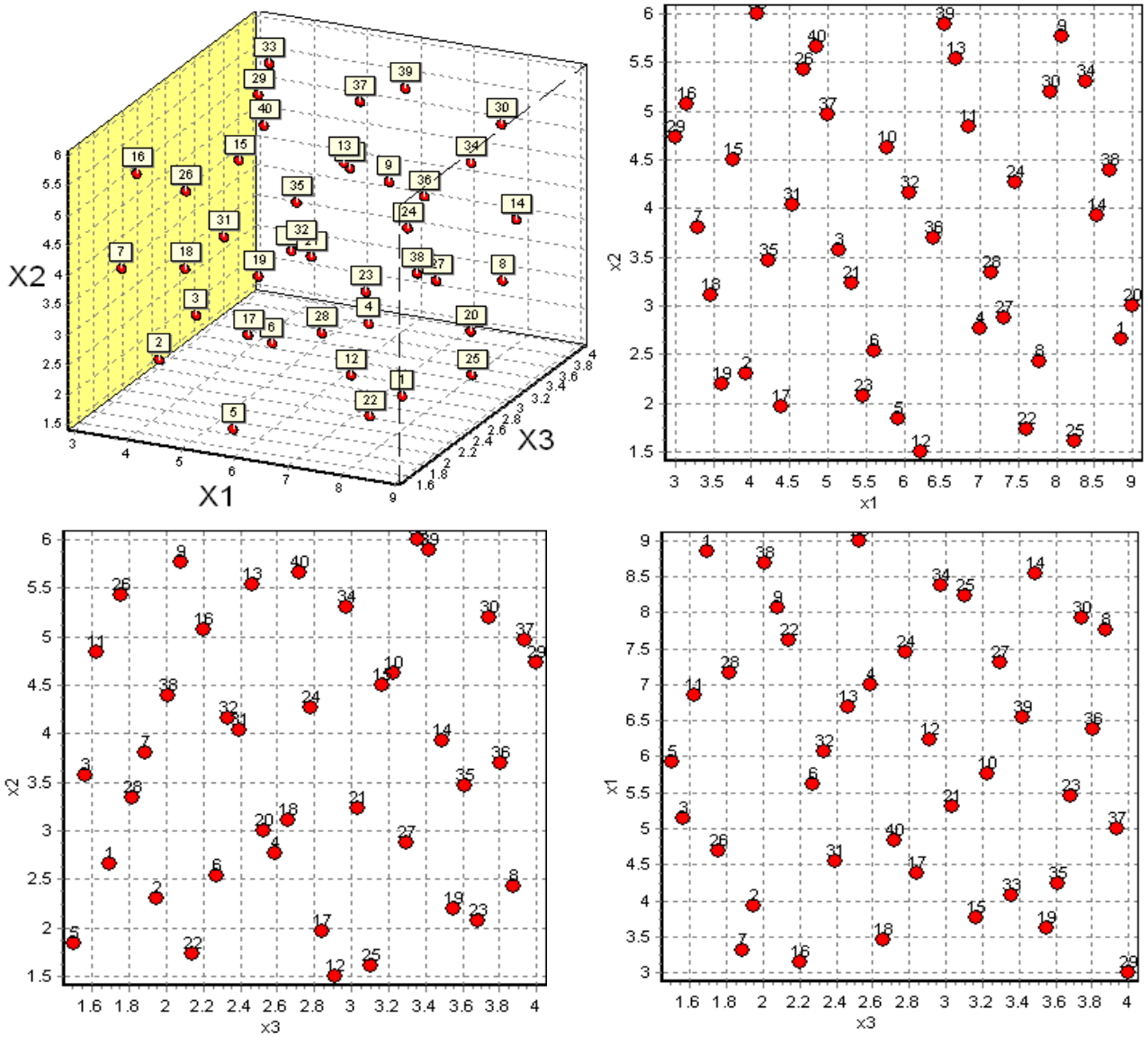

Fig. 16 Latin Hypercube design of experiment for 3 factors and 40 trial points (MSE criterion 0.313879).

$$\hat{y} = \beta_0 + \sum_{i=1}^{d} \beta_i x_i + \sum_{i=1}^{d-1} \sum_{j=i+1}^{d} \beta_{ij} x_i x_j + \sum_{i=1}^{d} \beta_{ij} x_i^2 + \varepsilon \quad (3)$$

where there are d variables $x_1, \ldots, x_d$, $L = (d+1)(d+2)/2$ unknown β coefficients and the errors ε are assumed independent with zero mean and constant variance σ_2. In case of local approximation coefficients $\beta = \beta_1, \beta_2, \beta_3, \ldots, \beta_L$ depend on point x_0 where prediction is calculated and are obtained by using weighted least squares:

$$\beta = \arg\min_{\beta} \sum_{j \in N_x} w(x_0 - x_j) \times (y_j - \hat{y}(x_j))^2 \quad (4)$$

where the significance of neighboring points in the set N_x is taken into account by Gaussian kernel:

$$w(u) = \exp\left(-\alpha u^2\right) \quad (5)$$

where u is Euclidian distance from x_0 to current point and α is coefficient that characterizes significance.

Quality of approximation is estimated by crossvalidation relative error:

$$\sigma_{err} = 100\% \frac{\sqrt{\frac{1}{n}\sum_{i=1}^{n} (\hat{y}_{-i}(x_i) - y_i)^2}}{\sqrt{\frac{1}{n-1}\sum_{i=1}^{n} (y_i - \bar{y})^2}} \quad (6)$$

where root mean squared prediction error stands in numerator and mean square deviation of response from its average value stands in denominator, n is a number

of confirmation points and $\sum_{i=1}^{n} \hat{y}_{-j}(x_i)$ denotes sum of responses calculated without taking into account j-th point. Leave one out crossvalidation method is used for calculation of Eq. (6).

Approximations of the responses show that best value of crossvalidation SigmaCross% (6) is obtained for the GP volume, then for the maximal displacement URES of the GP, fundamental frequency of the GP and then for the equivalent stresses $\sigma_{vonMises}$. The quality indices of approximations are shown in Table 2 for the responses y: 1 to 5 are equivalent stresses $\sigma_{vonMises}$ at the 5 predefined points of bracket (Fig. 17) and 6 is maximal displacement URES of the GP from strength calculation analysis; 7 is the GP volume; 8 is the fundamental frequency of the GP from frequency analysis. Some cross section graphs of the approximated responses are shown in Fig. 18.

Next, the problem of shape optimization of the bus GP brackets are defined as follows: Minimize the total volume V of the GP components with brackets subjected to constraints: (1) On the GP maximal displacement $URES$ < 1.5 mm; (2) on equivalent stresses $\sigma_{vonMises}$ at 5 points (Fig. 17) $\sigma_{vonMises} \leq 1.5$ MPa and 3) on fundamental frequency f>120 Hz.

Using locally weighted polynomial approximations of responses and global stochastic search procedure [12], realized in EDAOpt, the optimal shape of the GP brackets are obtained. The obtained smooth shapes of the GP brackets are shown in Fig. 19.

8. Conclusions

The most stressed regions of the GP are found by the strength analysis. The first 10 natural frequencies GP are computed. The results show high density of the natural frequencies in the frequency domain from 140 to 332 Hz. Some initial results of dynamic analysis of the GP are presented. The dynamic responses are calculated at the characteristic points of the GP devices. The harmonic analysis shows significance of the eighth

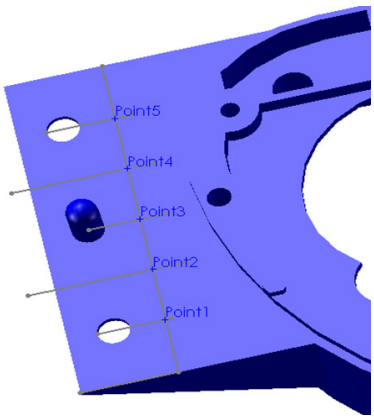

Fig. 17 Registration of equivalent stresses at 5 places on the GP bracket.

Table 2 Quality indices for approximations of responses.

Functions Yi:	MISES1	MISES2	MISES3	MISES4	MISES5	URES6	Volume7	Frequency8
Sigma cross	161215.860757	58020.948438	64115.843153	56586.633090	74981.381526	0.000004	9.874085	0.087050
Sigma Cross%	69.51 %	39.64 %	63.44 %	64.23 %	55.41 %	3.37%	0.69 %	3.54 %
Sigma	63477.457320	18979.912121	26788.443666	18252.960409	24791.255478	0.000001	2.668305	0.028257
Sigma%	27.368431	12.966346	26.506684	20.718825	18.319501	1.224116	0.185967	1.147957
Sigma0	74693.721588	22333.602062	31521.876229	21478.200301	29171.791257	0.000002	3.139786	0.033250
Sigma0%	32.204345	15.257458	31.190331	24.379775	21.556499	1.440413	0.218827	1.350798
Mean Exp. value	1029019.166667	693319.166667	599654.444444	761177.500000	1124560.555556	0.001647	168059.510483	62.352056
St. Dev. of Exp.	231936.782579	146378.260593	101062.975813	88098.435456	135327.131261	0.000120	1434.825935	2.461525
Exp. range	1066260.000000	630230.000000	404810.000000	351980.000000	632930.000000	0.000481	5172.534300	9.647000
Max error	201332.587785	53060.994863	-78647.746249	34487.289138	108809.431056	-0.000004	6.305461	-0.053774
Bad point No.	13	6	27	11	15	4	28	10
Max Rel. error	18.38 %	6.79 %	16.35 %	5.51 %	7.96 %	0.21 %	0.00 %	0.08 %
Bad Rel. point No.	13	9	27	36	15	4	28	10

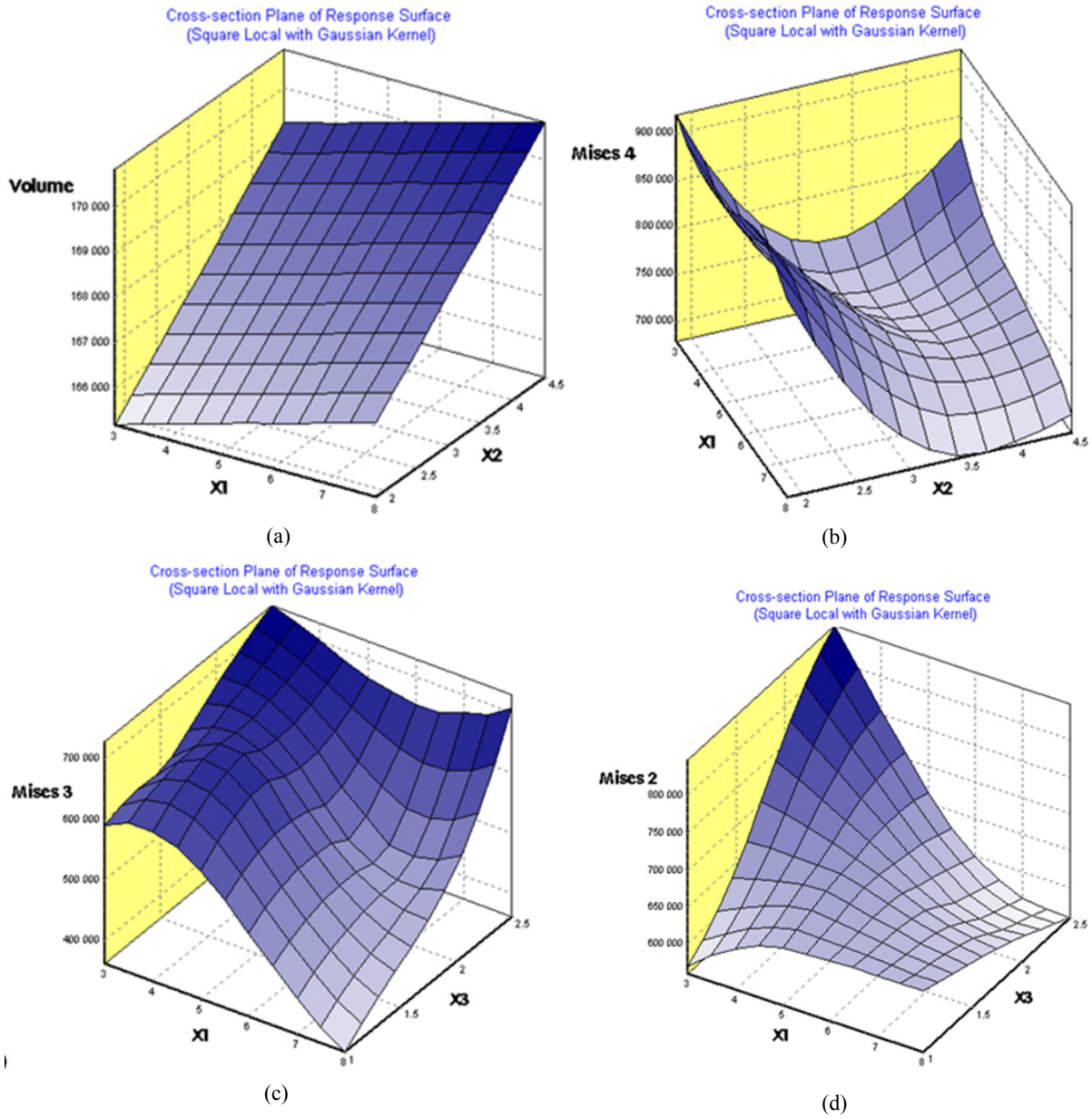

Fig. 18 Obtained functional dependences on design variables X1, X2 and X3: (a) volume and (b)-(d) maximal equivalent stresses $\sigma_{vonMises}$ at the points 2-4 (Fig. 17).

natural frequency that causes excessive vertical and horizontal displacements. The transient analysis of the GP is done in the case of polyharmonical excitations. The power spectral densities of the GP displacements and stresses at the characteristic points are found in the case of random excitations. The obtained responses are successfully used for the metamodels building based on local polynomial approximation. The shape optimization of the GP bracket is implemented using natural frequency that causes excessive vertical and horizontal displacements. The transient analysis of the GP is done in the case of polyharmonical excitations. The power spectral densities of the GP displacements and stresses at the characteristic points are found in the case of random excitations. The obtained responses are successfully used for the metamodels building based on local polynomial approximation. The shape optimization of the GP bracket is implemented using metamodels. The improved design of GP brackets with variable cross sections thickness is found, taking into

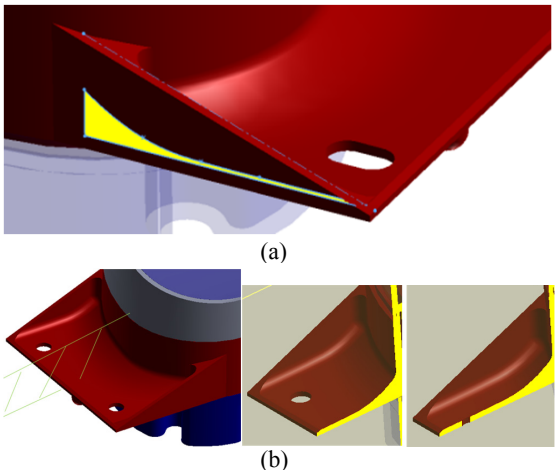

Fig. 19 Obtained shapes of the GP brackets: (a) shown on plane of the right bracket; (b) the left bracket and its cross sections at the middle and trough the hole.

account manufacturer requirements.

Acknowledgments

This work has been supported by the European Social Fund within the Project No. 2013/0025/1DP/1.1.1.2.0/13/APIA/VIAA/019 "New "Smart" Nanocomposite Materials for Roads, Bridges, Buildings and Transport Vehicle" and Project No. 2013/6/PVS ID1747 "KEDRO".

References

[1] A. Janushevskis, J. Auzins, A.G. Ancane, A. Melnikovs, J. Viba, Multiobjective optimization of automotive vehicle gage panel, in: Proceedings of the 10th International Conference on Vibration Problems, Prague, Czech Republic, Sept. 5-8, 2011, pp. 180-185.

[2] A. Janushevskis, J. Auzins, A. Melnikovs, A.G. Ancane, Shape optimization of mechanical components of measurement systems, in: Z. Haq (Ed.), Advanced Topics in Measurements, InTech, 2012, pp. 243-262.

[3] MIL-STD-810F, United States Military Standard, Environmental Engineering Considerations and Laboratory Tests, 2000.

[4] J.S. Arora, Introduction to Optimum Design, 2nd ed., Elsevier, 2004.

[5] M.P. Bendsoe, O. Sigmund, Topology Optimization: Theory, Methods and Application, 2nd ed., Springer, Heidelberg, Berlin, 2003.

[6] G.N. Vanderplaats, Numerical Optimization Techniques for Engineering Design with Applications, 4th ed., Vanderplaats Research & Development, Inc., Colorado Springs, CO, 2004.

[7] H. Mullerschon, N. Lazarov, K. Witowski, Application of topology optimization for crash with LC-OPT/topology, in: Proc. 11th Int. LS-DYNA Users Conference, 2010, pp. 17-46.

[8] J. Janusevskis, R.L. Riche, Simultaneous Kriging-Based Sampling for Optimization and Uncertainty Propagation, Technical Report [Hal- 00506957], 2010.

[9] J. Auzins, J. Janushevskis, A. Janushevskis, K. Kalnins, Optimisation of designs for natural and numerical experiments, in: Extended Abstracts of the 6th Int. ASMO-UK/ISSMO Conference on Engineering Design Optimization, Oxford, UK, 2006, pp. 118-121.

[10] J. Auzins, A. Janushevskis, J. Janushevskis, Optimized experimental designs for metamodeling: Algorithm, Scientific Journal of RTU: Transport and Engineering Mechanics 33 (2010) 25-29.

[11] J. Auzins, A. Janushevskis, Design of Experiments and Analysis, Riga, 2007.

[12] A. Janushevskis, T. Akinfiev, J. Auzins, A. Boyko, A comparative analysis of global search procedures, Estonian Acad. Sci. Eng. 10 (4) (2004) 235-250.